Stabilization of Power Networks via Market Dynamics

Pengcheng You
Zhejiang University
pcyou@zju.edu.cn

John Z.F. Pang
California Institute of Technology
jzpang@caltech.edu

Enoch Yeung
Pacific Northwest National Laboratory
enoch.yeung@pnnl.gov

ABSTRACT

This work investigates the increasing interactions between power network dynamics and market dynamics. A dynamical spot pricing mechanism for rational market behavior of generators and loads is designed to model market dynamics, which provably drives a power network to an equilibrium operating point, achieving secondary frequency control and economic dispatch.

1 INTRODUCTION

An ideal power network operates at nominal frequency and remains stable at an equilibrium where overall power production matches consumption. However, fluctuations at both supply and demand sides cause frequency deviation. If not well addressed, this may propagate across the network and lead to potential blackouts. Generally, frequency regulation is realized in three stages of generation-side control: (i) Primary: droop control [17] - frequency stabilization; (ii) Secondary: automatic generation control (AGC) [7] - frequency restoration; (iii) Tertiary: economic dispatch - generation and power flow scheduling. Recently, there has also been emerging interest in designing load-side frequency controllers [9, 11, 14, 15, 18, 19].

Both primary and secondary stages require direct control of generators or loads acquired from an early ancillary service market. The tertiary stage relies on a power market to determine dispatch. With the increasing low-inertia dispatchable units in the power system, the frequency of market updates for economic efficiency may result in a confluence of the actions of secondary and tertiary control. This confluence is advantageous in two ways. Firstly, real-time power imbalance can be offset in an *ex-post* power market that is more economically efficient. Secondly, market updates take into account physical responses of the power system and thus reduce modeling uncertainty.

The concept of market dynamics is first proposed in [1] where a dynamic uniform pricing mechanism is designed to measure global energy imbalance. A lot of work adopts similar pricing designs [3, 5, 10, 16], but neglects spatially-variant values of electricity due to network congestion. [4, 8, 12, 13] extend the market model to involve nodal pricing. However, their nodal prices result from the introduction of *virtual flow* variables and fail to capture the economic interpretation of locational marginal prices (LMPs).

In this work we propose a compatible model of market dynamics based on linearized swing equations. We introduce a precise dynamical spot pricing mechanism to account for both power imbalance and line congestion. Further, we model market participants as rational agents that respond to price changes by maximizing their local utility. We prove that a controller based on market dynamics is able to balance power, restore the frequency to its nominal value and maintain line flows within thermal limits at equilibrium.

e-Energy'18, June 12–15, 2018, Karlsruhe, Germany

ACM ISBN 978-1-4503-5767-8/18/06…$15.00
https://doi.org/10.1145/3208903.3208916

2 MODEL

Let $\mathbb{R}$ ($\mathbb{R}_+$ and $\mathbb{R}_-$) be the set of (positive and negative) real numbers and $\mathbb{N}$ be the set of natural numbers. For a finite set $\mathcal{H} \subset \mathbb{N}$, its cardinality is denoted as $|\mathcal{H}|$. For a set of scalar variables $y_j, j \in \mathcal{H}$, its column vector is denoted as $y_{\mathcal{H}}$. Sometimes the subscript $\mathcal{H}$ is dropped if the set is clear from the context. Given vectors y and u, we define an element-wise projection $[y]_u^+$ where $[y_j]_{u_j}^+ = y_j$ if $y_j > 0$ or $u_j > 0$, and $[y_j]_{u_j}^+ = 0$ otherwise. For a matrix Y, Y^T denotes its transpose. Let Y_j be the jth row of Y and $Y_{\mathcal{H}}$ be submatrix of Y composed of all the rows $Y_j, j \in \mathcal{H}$. We may use 1 or 0 to denote a column vector of all 1's or 0's if its dimension is clear without ambiguity.

2.1 Power network

Consider a structure-preserving power network with a connected directed graph $(\mathcal{N}, \mathcal{E})$, where $\mathcal{N} := \{0, 1, \ldots, |\mathcal{N}| - 1\}$ is the set of nodes and $\mathcal{E} \subset \mathcal{N} \times \mathcal{N}$ is the set of edges connecting nodes. Each node represents a bus and each edge is a transmission line. The buses in $\mathcal{N}$ are partitioned into three categories $\mathcal{N} = \mathcal{G} \cup \mathcal{L} \cup \{0\}$ where $\mathcal{G}$ and $\mathcal{L}$ are the sets of generator and load buses, respectively. Note that a generator bus can also have local loads. For notational convenience, assume bus 0 is a pure slack bus and each generator bus has only one (aggregate) generator and one (aggregate) load while each load bus has just one (aggregate) load. Let $\mathcal{N}^+ := \mathcal{N} \backslash \{0\} = \mathcal{G} \cup \mathcal{L}$. We use (j, k) to denote the line from bus j to bus k. An arbitrary orientation is applied such that if $(j, k) \in \mathcal{E}$ then $(k, j) \notin \mathcal{E}$. Each line $(j, k) \in \mathcal{E}$ is endowed with an impedance z_{jk}.

Define the incidence matrix $C \in \mathbb{R}^{|\mathcal{N}| \times |\mathcal{E}|}$ for the network graph where its element $C_{j,e} = 1$ if $e = (j, k) \in \mathcal{E}$, $C_{j,e} = -1$ if $e = (k, j) \in \mathcal{E}$ and $C_{j,e} = 0$ otherwise. Meanwhile, define $\bar{C} \in \mathbb{R}^{(|\mathcal{N}|-1) \times |\mathcal{E}|}$ based on C by eliminating the row that corresponds to the slack bus to remove dependency. Several standard assumptions for a linear transmission network model are applied [6]: 1) the voltage magnitude $|V_j|$ is constant for each bus $j \in \mathcal{N}$; 2) each line $(j, k) \in \mathcal{E}$ is lossless, i.e., $z_{jk} := \mathbf{i} x_{jk}$ where x_{jk} is a reactance; 3) reactive power injections and flows are all ignored. These assumptions are milder than those made in the standard DC approximation of power flow equations since the nominal phase angle difference across each line is not necessarily small and trigonometric nonlinearities are still modeled.

On this premise, the network dynamics are characterized by

$$\dot{\theta} = \omega \tag{1a}$$

$$M\dot{\omega}_{\mathcal{G}} = r_{\mathcal{G}} + p - d_{\mathcal{G}} - D_{\mathcal{G}}\omega_{\mathcal{G}} - C_{\mathcal{G}}B\bar{C}^T\theta_{\mathcal{N}^+} \quad (1b)$$

$$0 = r_{\mathcal{L}} - d_{\mathcal{L}} - D_{\mathcal{L}}\omega_{\mathcal{L}} - C_{\mathcal{L}}B\bar{C}^T\theta_{\mathcal{N}^+} \quad (1c)$$

$$0 = r_0 - D_0\omega_0 - C_0B\bar{C}^T\theta_{\mathcal{N}^+} \quad (1d)$$

where $\theta := (\theta_j, j \in \mathcal{N})$ denote the bus phase angles, $\omega := (\omega_j, j \in \mathcal{N})$ denote the bus frequencies, $p := (p_j, j \in \mathcal{G})$ denote the outputs of generators, and $d := (d_j, j \in \mathcal{N}^+)$ denote elastic loads. $M := \mathrm{diag}(M_j, j \in \mathcal{G})$ are generators' inertia, $r := (r_j, j \in \mathcal{N})$ are constant step changes of net power injections at buses, i.e., instant power imbalance, $D := \mathrm{diag}(D_j, j \in \mathcal{N})$ are constants representing generator damping or uncontrollable frequency-dependent loads, and $B := \mathrm{diag}(B_{jk}, (j,k) \in \mathcal{E})$ are line parameters that characterize the sensitivity of each line flow to its two-end phase angle difference (see the derivation of B in Appendix A.1). Here all the state variables θ and ω are *deviations* from their nominal values. (1a)-(1d) describe the nodal swing dynamics. Let $\tilde{\theta} := \bar{C}^T\theta_{\mathcal{N}^+} \in \mathbb{R}^{|\mathcal{E}|}$. Since $\bar{C}^T$ is full column rank, there is a bijection between $\theta_{\mathcal{N}^+}$ and $\tilde{\theta}$. In the sequel we will use both interchangeably.

2.2 Power market

The power network operates as per a schedule determined in an *ex-ante* power market, day ahead or hour ahead, at a large timescale. However, generations or loads cannot avoid deviating from scheduled values in real time due to unexpectedness, causing power imbalance in the network. The imbalance will drive the frequency away from its nominal value and, if not timely eliminated, may deteriorate or even disrupt the whole system.

Instead of the conventional regulation services that may idle unnecessary power reserves, we resort to a dynamical *ex-post* power market as a lever for secondary frequency control and congestion management. We assume a fully competitive market, i.e., no strategic market participant is able to exercise market power. Such a market is economically efficient in terms of social welfare in nature where each participant, a generator or a load, is an individual price-taker and rationally minimizes its net cost.

We model the dynamical behavior of the market participants by

$$T^p\dot{p} = -p + p^C - R^{-1}\omega_{\mathcal{G}} \quad (1e)$$

$$T^d\dot{d} = -d + d^C \quad (1f)$$

where $T^p := \mathrm{diag}(T^p_j, j \in \mathcal{G})$, $T^d := \mathrm{diag}(T^d_j, j \in \mathcal{N}^+)$ are time constants and $R := \mathrm{diag}(R_j, j \in \mathcal{G})$ are the droop parameters. p^C and d^C are self-control commands for generators and loads, respectively. (1e) captures a simplified turbine dynamical model for generators, and likewise (1f) mimics the load dynamics. Note that p, d could be deviations from scheduled values or new generations and loads, which are presumably responsive in the *ex-post* power market.

A power market is distinguished from other generic markets in that it is a networked market governed by Kirchhoff's laws. The commodity in the market, i.e., electricity, is indiscriminate itself but cannot freely be transmitted and distributed in a multilateral trade. Physical laws as well as transmission capabilities constrain market operation and impose spatially variant values on electricity, i.e., LMPs. Specifically, a static power market aims to solve a canonical DC economic dispatch problem (EDP) with line thermal constraints:
EDP-1:

$$\min_{p,d,\theta_{\mathcal{N}^+}} \quad \sum_{j\in\mathcal{G}} J_j(p_j) - \sum_{j\in\mathcal{N}^+} U_j(d_j) \quad (2a)$$

$$\text{s.t.} \quad r_{\mathcal{G}} + p - d_{\mathcal{G}} - C_{\mathcal{G}}B\bar{C}^T\theta_{\mathcal{N}^+} = 0 \quad (2b)$$

$$r_{\mathcal{L}} - d_{\mathcal{L}} - C_{\mathcal{L}}B\bar{C}^T\theta_{\mathcal{N}^+} = 0 \quad (2c)$$

$$r_0 - C_0B\bar{C}^T\theta_{\mathcal{N}^+} = 0 \quad (2d)$$

$$\underline{F} \le B\bar{C}^T\theta_{\mathcal{N}^+} \le \overline{F} \quad (2e)$$

where $J_j(\cdot) : \mathbb{R} \to \mathbb{R}$ and $U_j(\cdot) : \mathbb{R} \to \mathbb{R}$ are the cost function of a generator and the utility function of a load, respectively[1]. Assume $J_j(\cdot)$ and $U_j(\cdot)$ are strictly convex and concave, respectively, and continuously differentiable. $\underline{F}$ and $\overline{F}$ are the lower and upper thermal limits on line flows, respectively. Basically (2a) aims to minimize social cost (maximize social welfare) across the market. We make the common assumption that EDP-1 is feasible and finite.

Define $\pi := (\pi_j, j \in \mathcal{N})$ as the net power injections at all buses. Accordingly $\pi_{\mathcal{G}} = r_{\mathcal{G}} + p - d_{\mathcal{G}}$ and $\pi_{\mathcal{L}} = r_{\mathcal{L}} - d_{\mathcal{L}}$. From (2b) and (2c), $\pi_{\mathcal{N}^+} = \bar{C}B\bar{C}^T\theta_{\mathcal{N}^+}$, or equivalently $\theta_{\mathcal{N}^+} = (\bar{C}B\bar{C}^T)^{-1}\pi_{\mathcal{N}^+}$ since B is diagonal and $\bar{C}^T$ is full column rank. Let $H^T := B\bar{C}^T(\bar{C}B\bar{C}^T)^{-1} \in \mathbb{R}^{|\mathcal{E}|\times(|\mathcal{N}|-1)}$ be the *power injection shift matrix* of the power network, then (2) can be equivalently rewritten as
EDP-2:

$$\min_{p,d} \quad \sum_{j\in\mathcal{G}} J_j(p_j) - \sum_{j\in\mathcal{N}^+} U_j(d_j) \quad (3a)$$

$$\text{s.t.} \quad \mathbf{1}^T_{\mathcal{G}}(r_{\mathcal{G}} + p - d_{\mathcal{G}}) + \mathbf{1}^T_{\mathcal{L}}(r_{\mathcal{L}} - d_{\mathcal{L}}) + r_0 = 0 \quad (3b)$$

$$H^T_{\mathcal{G}}(r_{\mathcal{G}} + p - d_{\mathcal{G}}) + H^T_{\mathcal{L}}(r_{\mathcal{L}} - d_{\mathcal{L}}) \ge \underline{F} \quad (3c)$$

$$H^T_{\mathcal{G}}(r_{\mathcal{G}} + p - d_{\mathcal{G}}) + H^T_{\mathcal{L}}(r_{\mathcal{L}} - d_{\mathcal{L}}) \le \overline{F} \quad (3d)$$

where (3b) imposes global power balance and (3c), (3d) separately redescribe line flows with respect to nodal net power injections.

Introduce dual variables $\lambda \in \mathbb{R}, \eta^- \in \mathbb{R}^{|\mathcal{E}|}_+$ and $\eta^+ \in \mathbb{R}^{|\mathcal{E}|}_+$ for (3b), (3c) and (3d), respectively, and suppose (p^*, d^*) and $(\lambda^*, \eta^{-*}, \eta^{+*})$ are primal-dual optimum, then canonical LMPs across buses $j \in \mathcal{N}^+$ are defined as $\lambda^*\mathbf{1}_{\mathcal{N}^+} - H\eta^{-*} + H\eta^{+*}$, which can also be interpreted as *weighted shadow prices* in terms of (3b)-(3d). Given the LMPs, (p^*, d^*), a market equilibrium that balances supply and demand as well as maximizes social welfare, can be achieved by rational market participants individually.

3 MARKET DYNAMICS

The control commands p^C and d^C in (1) are to be designed which should reflect the rational market behavior of individual generators and loads. In this section we describe a controller based on market dynamics inspired by LMPs, present the underlying rationale, and prove its ability to stabilize the power network.

3.1 Controller design

In particular, we characterize the market dynamics by

$$\dot{\lambda} = \gamma^\lambda\left(-\mathbf{1}^T_{\mathcal{G}}(r_{\mathcal{G}} + p - d_{\mathcal{G}}) - \mathbf{1}^T_{\mathcal{L}}(r_{\mathcal{L}} - d_{\mathcal{L}}) - r_0\right) \quad (4a)$$

$$\dot{\eta}^- = \Gamma^{\eta^-}\left[\underline{F} - H^T_{\mathcal{G}}(r_{\mathcal{G}} + p - d_{\mathcal{G}}) - H^T_{\mathcal{L}}(r_{\mathcal{L}} - d_{\mathcal{L}})\right]^+_{\eta^-} \quad (4b)$$

$$\dot{\eta}^+ = \Gamma^{\eta^+}\left[H^T_{\mathcal{G}}(r_{\mathcal{G}} + p - d_{\mathcal{G}}) + H^T_{\mathcal{L}}(r_{\mathcal{L}} - d_{\mathcal{L}}) - \overline{F}\right]^+_{\eta^+} \quad (4c)$$

$$p^C_j = \lambda - \omega_j + H_j\eta^- - H_j\eta^+ - J'_j(p_j) + p_j + \frac{\omega_j}{R_j}, \quad j \in \mathcal{G} \quad (4d)$$

$$d^C_j = U'_j(d_j) - \lambda + \omega_j - H_j\eta^- + H_j\eta^+ + d_j, \quad j \in \mathcal{N}^+ \quad (4e)$$

[1]For simplicity we ignore the capacities of generators and loads, which can be implicitly imposed by property design of cost/utility functions [9]. Note that the capacity constraints can also be incorporated through a projection method, see [14, 15].

where $\gamma^{\lambda}, \Gamma^{\eta^-} := \text{diag}(\gamma_j^{\eta^-}, j \in \mathcal{E})$ and $\Gamma^{\eta^+} := \text{diag}(\gamma_j^{\eta^+}, j \in \mathcal{E})$ are positive constants or diagonal constant matrices. (4a)-(4c) are the dynamics of dual Lagrange multipliers and proxies for the costs of constraint violation. (4d), (4e) are adjustments of control commands for generators and loads based on market updates. Specifically, we define $\lambda - \omega + H\eta^- - H\eta^+$ as *dynamical locational marginal prices (DLMPs)*, where λ (resp. $-\omega$) prices global (resp. local) power imbalance, and $H\eta^- - H\eta^+$ prices line congestion. From (1b) and (4a)-(4c), DLMPs are spatial-temporal variants that precisely embody market evolution in response to real-time states of the power network. Then (4d), (4e) combined with (1d), (1e) reveal a direct economic interpretation that a generator (load) tends to augment (reduce) production (consumption) if the DLMP exceeds its marginal cost (utility); otherwise, it will curtail (increase) production (consumption). This matches exactly with the rational behavior of market participants.

To avoid measuring the power imbalance r, we can utilize (1b)-(1d) to have replacements for $r_{\mathcal{G}} + p - d_{\mathcal{G}}$, $r_{\mathcal{L}} - d_{\mathcal{L}}$ and r_0 since θ, ω and $\dot{\omega}$ are readily observable in the current power system operation. We highlight the controller implementation: (4a)-(4c) require the local measurements of ω_j, $\dot{\omega}_j$ and θ_j at each bus as well as $(\theta_k, k : (j,k) \in \mathcal{E}$ or $(k,j) \in \mathcal{E})$ from all its neighbor buses through neighborhood communications. (4d), (4e) necessitate the bidirectional communication between each bus and a central market operator to exchange system state information and DLMPs, which can build on the existing market communication topologies.

3.2 Underlying algorithm

The market dynamics controller (4) is derived from a partial primal-dual algorithm on the following problem:
EDP-3:

$$\min_{p,d,\tilde{\theta},\omega} \quad \sum_{j\in\mathcal{G}} J_j(p_j) - \sum_{j\in\mathcal{N}^+} U_j(d_j) + \sum_{j\in\mathcal{N}} \frac{D_j}{2}\omega_j^2 \tag{5a}$$

$$\text{s.t.} \quad r_{\mathcal{G}} + p - d_{\mathcal{G}} - D_{\mathcal{G}}\omega_{\mathcal{G}} - C_{\mathcal{G}}B\tilde{\theta} = 0 \tag{5b}$$

$$r_{\mathcal{L}} - d_{\mathcal{L}} - D_{\mathcal{L}}\omega_{\mathcal{L}} - C_{\mathcal{L}}B\tilde{\theta} = 0 \tag{5c}$$

$$r_0 - D_0\omega_0 - C_0B\tilde{\theta} = 0 \tag{5d}$$

$$\mathbf{1}_{\mathcal{G}}^T(r_{\mathcal{G}} + p - d_{\mathcal{G}}) + \mathbf{1}_{\mathcal{L}}^T(r_{\mathcal{L}} - d_{\mathcal{L}}) + r_0 = 0 \tag{5e}$$

$$H_{\mathcal{G}}^T(r_{\mathcal{G}} + p - d_{\mathcal{G}}) + H_{\mathcal{L}}^T(r_{\mathcal{L}} - d_{\mathcal{L}}) \geq \underline{F} \tag{5f}$$

$$H_{\mathcal{G}}^T(r_{\mathcal{G}} + p - d_{\mathcal{G}}) + H_{\mathcal{L}}^T(r_{\mathcal{L}} - d_{\mathcal{L}}) \leq \overline{F} \tag{5g}$$

At first sight, EDP-3 seems a combination of EDP-1 and EDP-2. Similarly, we introduce dual variables $\mu_{\mathcal{G}} \in \mathbb{R}^{|\mathcal{G}|}$, $\mu_{\mathcal{L}} \in \mathbb{R}^{|\mathcal{L}|}$, $\mu_0 \in \mathbb{R}$, $\lambda \in \mathbb{R}$, $\eta^- \in \mathbb{R}_+^{|\mathcal{E}|}$ and $\eta^+ \in \mathbb{R}_+^{|\mathcal{E}|}$ for (5b)-(5g), respectively. For compactness, let $x := (p, d, \tilde{\theta}, \omega) \in \mathbb{R}^{|\mathcal{G}|+2|\mathcal{N}|+|\mathcal{E}|-1}$, $\nu := (\mu, \lambda) \in \mathbb{R}^{|\mathcal{N}|+1}$ and $\eta := (\eta^-, \eta^+) \in \mathbb{R}_+^{2|\mathcal{E}|}$. Then the Lagrangian of EDP-3 can be noted down as

$$\begin{aligned} L(x,\nu,\eta) := & \sum_{j\in\mathcal{G}} J_j(p_j) - \sum_{j\in\mathcal{N}^+} U_j(d_j) + \sum_{j\in\mathcal{N}} \frac{D_j}{2}\omega_j^2 \\ & + \mu_{\mathcal{G}}^T\left(r_{\mathcal{G}} + p - d_{\mathcal{G}} - D_{\mathcal{G}}\omega_{\mathcal{G}} - C_{\mathcal{G}}B\tilde{\theta}\right) \\ & + \mu_{\mathcal{L}}^T\left(r_{\mathcal{L}} - d_{\mathcal{L}} - D_{\mathcal{L}}\omega_{\mathcal{L}} - C_{\mathcal{L}}B\tilde{\theta}\right) + \mu_0\left(r_0 - D_0\omega_0 - C_0B\tilde{\theta}\right) \\ & + \lambda\left(-\mathbf{1}_{\mathcal{G}}^T(r_{\mathcal{G}} + p - d_{\mathcal{G}}) - \mathbf{1}_{\mathcal{L}}^T(r_{\mathcal{L}} - d_{\mathcal{L}}) - r_0\right) \\ & + \eta^{-T}\left(\underline{F} - H_{\mathcal{G}}^T(r_{\mathcal{G}} + p - d_{\mathcal{G}}) - H_{\mathcal{L}}^T(r_{\mathcal{L}} - d_{\mathcal{L}})\right) \\ & + \eta^{+T}\left(H_{\mathcal{G}}^T(r_{\mathcal{G}} + p - d_{\mathcal{G}}) + H_{\mathcal{L}}^T(r_{\mathcal{L}} - d_{\mathcal{L}}) - \overline{F}\right) \end{aligned} \tag{6}$$

We also assume that EDP-3 is feasible and finite, which is actually implied by the feasibility and finiteness of EDP-1, as we will show later. This assumption allows us to use the Karush-Kuhn-Tucker (KKT) conditions to characterize the optimality of EDP-3:

Theorem 3.1. *(x^*, ν^*, η^*) is a primal-dual optimal solution to EDP-3 if and only if $p^*, d^*, \tilde{\theta}^*$ are primal feasible, $\eta^{-*}, \eta^{+*} \geq 0$, and*

$$\mu^* = \omega^* = 0 \tag{7a}$$

$$p_j^* = J_j'^{-1}(\lambda^* - \omega_j^* + H_j\eta^{-*} - H_j\eta^{+*}), \quad j \in \mathcal{G} \tag{7b}$$

$$d_j^* = U_j'^{-1}(\lambda^* - \omega_j^* + H_j\eta^{-*} - H_j\eta^{+*}), \quad j \in \mathcal{N}^+ \tag{7c}$$

$$\text{diag}(\eta^{-*})\left(\underline{F} - H_{\mathcal{G}}^T(r_{\mathcal{G}} + p^* - d_{\mathcal{G}}^*) - H_{\mathcal{L}}^T(r_{\mathcal{L}} - d_{\mathcal{L}}^*)\right) = 0 \tag{7d}$$

$$\text{diag}(\eta^{+*})\left(H_{\mathcal{G}}^T(r_{\mathcal{G}} + p^* - d_{\mathcal{G}}^*) + H_{\mathcal{L}}^T(r_{\mathcal{L}} - d_{\mathcal{L}}^*) - \overline{F}\right) = 0 \tag{7e}$$

where $J_j'^{-1}(\cdot)$ and $U_j'^{-1}(\cdot)$ are the inverse functions of the derivatives of $J_j(\cdot)$ and $U_j(\cdot)$, respectively.

Note that by definition, $J_j'^{-1}(\cdot)$ and $U_j'^{-1}(\cdot)$ are both continuous and monotone. With Theorem 3.1, EDP-3 is indeed an equivalent of EDP-1 and EDP-2, which is formalized as

Theorem 3.2. *Given a vector $(p^*, d^*, \tilde{\theta}^*, \omega^*)$ that satisfies $\omega^* = 0$, $\tilde{\theta}^* = \bar{C}^T\theta_{\mathcal{N}^+}^*$ and $\pi_{\mathcal{N}^+}^* = \bar{C}B\bar{C}^T\theta_{\mathcal{N}^+}^*$ where $\pi_{\mathcal{G}}^* = r_{\mathcal{G}} + p^* - d_{\mathcal{G}}^*$ and $\pi_{\mathcal{L}}^* = r_{\mathcal{L}} - d_{\mathcal{L}}^*$, the following statements are equivalent:*

- *$(p^*, d^*, \theta_{\mathcal{N}^+}^*)$ is an optimal solution to EDP-1;*
- *(p^*, d^*) is an optimal solution to EDP-2;*
- *$(p^*, d^*, \tilde{\theta}^*, \omega^*)$ is an optimal solution to EDP-3.*

Theorem 3.2 allows us to look at EDP-3 as a proxy for EDP-1. Let

$$L(\tilde{x}, \nu, \eta) := \min_{\omega} L(x, \nu, \eta) \tag{8}$$

where $\tilde{x} := (p, d, \tilde{\theta}) \in \mathbb{R}^{|\mathcal{G}|+|\mathcal{N}|+|\mathcal{E}|-1}$. From (6), the minimization over ω basically aligns ω with μ, therefore

$$\begin{aligned} L(\tilde{x}, \nu, \eta) := & \sum_{j\in\mathcal{G}}\left[J_j(p_j) - (\lambda - \mu_j + H_j\eta^- - H_j\eta^+)p_j\right] \\ & - \sum_{j\in\mathcal{N}^+}\left[U_j(d_j) - (\lambda - \mu_j + H_j\eta^- - H_j\eta^+)d_j\right] \\ & - \sum_{j\in\mathcal{N}}\left[(\lambda - \mu_j + H_j\eta^- - H_j\eta^+)r_j + \frac{D_j}{2}\mu_j^2\right] \\ & - \tilde{\theta}^T BC^T\mu + \underline{F}^T\eta^- - \overline{F}^T\eta^+ \end{aligned} \tag{9}$$

which is strictly concave in μ. Consider

$$L(\tilde{x}, \tilde{\nu}, \eta) := \max_{\mu_{\mathcal{L}}, \mu_0} L(\tilde{x}, \nu, \eta) \tag{10}$$

where $\tilde{\nu} := (\mu_{\mathcal{G}}, \lambda) \in \mathbb{R}^{|\mathcal{G}|+1}$. The minimizers $\mu_{\mathcal{L}}^*(\tilde{x}, \tilde{\nu}, \eta)$ and $\mu_0^*(\tilde{x}, \tilde{\nu}, \eta)$ are unique due to the strict concavity and $L(\tilde{x}, \tilde{\nu}, \eta)$ remains strictly concave in $\mu_{\mathcal{G}}$.

The standard primal-dual gradient algorithm in the continuous time domain for $L(\tilde{x}, \tilde{\nu}, \eta)$ is

$$\dot{\tilde{x}} = -\Gamma^{\tilde{x}}\nabla_{\tilde{x}}L(\tilde{x}, \tilde{\nu}, \eta) \tag{11a}$$

$$\dot{\tilde{\nu}} = \Gamma^{\tilde{\nu}}\nabla_{\tilde{\nu}}L(\tilde{x}, \tilde{\nu}, \eta) \tag{11b}$$

$$\dot{\eta} = \Gamma^{\eta}\left[\nabla_{\eta}L(\tilde{x}, \tilde{\nu}, \eta)\right]_{\eta}^+ \tag{11c}$$

where $\Gamma^{\tilde{x}} := \text{diag}(\gamma_j^p, j \in \mathcal{G}, \gamma_j^d, j \in \mathcal{N}^+, \gamma_{jk}^{\tilde{\theta}}, (j,k) \in \mathcal{E})$, $\Gamma^{\tilde{\nu}} := \text{diag}(\gamma_j^{\mu}, j \in \mathcal{G}, \gamma^{\lambda})$ and $\Gamma^{\eta} := \text{diag}(\gamma_j^{\eta^-}, j \in \mathcal{E}, \gamma_j^{\eta^+}, j \in \mathcal{E})$ are positive constants or diagonal constant matrices. Note that μ plays the role of the absent frequency ω above. Therefore, the procedures (8), (10) and (11) correspond to the closed-loop system of the power network dynamics (1) with the market dynamics controller (4). In

particular, (8) enforces $\omega \equiv \mu$, and the unique minimizers of (10) must satisfy $\frac{\partial L}{\partial \mu_{\mathcal{L}}}(\tilde{x}, \nu, \eta) = 0$ and $\frac{\partial L}{\partial \mu_0}(\tilde{x}, \nu, \eta) = 0$, which jointly amount to (1c) and (1d). The λ-part of (11b) and (11c) are exactly (4a)-(4c) in our controller. Let $\gamma_j^p = 1/T_j^p$, $j \in \mathcal{G}$, and $\gamma_j^d = 1/T_j^d$, $j \in \mathcal{N}^+$, then the p, d-parts of (11a) appear when the control commands (4d), (4e) are applied to the generator and load dynamics (1e), (1f). Moreover, the $\tilde{\theta}$-part of (11a) and the $\mu_{\mathcal{G}}$-part of (11b) are automatically carried out by the power network dynamics (1a) and (1b) by setting $\gamma_{jk}^{\tilde{\theta}} = 1/B_{jk}$, $(j,k) \in \mathcal{E}$, and $\gamma_j^{\mu} = 1/M_j$, $j \in \mathcal{G}$.

The closed-loop system (1) and (4) represents a typical cyber-physical system and implements an underlying partial primal-dual gradient algorithm that solves EDP-3, an equivalent variant of the market-clearing EDP-1. This embodies a market-aware controller design as (4).

3.3 System stability

We formally show the market dynamics controller (4) is able to stabilize the power network dynamics (1), i.e., eliminate power imbalance, restore the nominal frequency, and maintain line flows within thermal limits at equilibrium. First, define

$$\mathbb{I} := \left\{ (\tilde{x}, \tilde{\nu}, \eta) \mid \tilde{x} \in \mathbb{R}^{|\mathcal{G}|+|\mathcal{N}|+|\mathcal{E}|-1},\ \tilde{\nu} \in \mathbb{R}^{|\mathcal{G}|+1},\ \eta \in \mathbb{R}_+^{2|\mathcal{E}|} \right\}$$

The equilibrium of the closed-loop system (1) and (4) starting from any initial point in $\mathbb{I}$ is characterized by the following theorem.

Theorem 3.3. *For the closed-loop system* (1) *and* (4) *starting from any initial point in* $\mathbb{I}$*, a trajectory point* $(p^*, d^*, \theta^*, \omega^*, \lambda^*, \eta^{-*}, \eta^{+*})$ *is its equilibrium if and only if* $(p^*, d^*, \tilde{\theta}^*, \omega^*, \mu^*, \lambda^*, \eta^{-*}, \eta^{+*})$ *is a primal-dual optimal solution to EDP-3 with* $\tilde{\theta}^* = C^T \theta^*$ *and* $\omega^* = \mu^*$.

Corollary 3.4. *Every equilibrium point optimally solves EDP-3, or equivalently EDP-1, which clears the ex-post power market in an economically efficient way. Meanwhile, power balance is reestablished over the network and the frequency is driven back to its nominal value with line thermal constraints satisfied.*

Next we proceed to show that given the initial condition of $\mathbb{I}$, the closed-loop system indeed converges to one equilibrium point.

Define $\mathbb{E} := \left\{ (\tilde{x}, \tilde{\nu}, \eta) \mid \dot{\tilde{x}} = 0,\ \dot{\tilde{\nu}} = 0,\ \dot{\eta} = 0 \right\}$ as the set of equilibrium points of (11) with initial points in $\mathbb{I}$. Any point $(\tilde{x}, \tilde{\nu}, \eta) \in \mathbb{E}$ also implies a unique equilibrium point of (1) and (4) with $\mu_{\mathcal{L}}^*(\tilde{x}, \tilde{\nu}, \eta)$, $\mu_0^*(\tilde{x}, \tilde{\nu}, \eta)$ and $\omega = \mu$, which also characterizes a primal-dual optimal solution to EDP-3 by Theorem 3.3. Then we are able to conclude the following theorem:

Theorem 3.5. *The equilibrium set* $\mathbb{E}$ *of* (11) *is asymptotically stable. In particular, starting from any initial point* $(\tilde{x}(0), \tilde{\nu}(0), \eta(0)) \in \mathbb{I}$, $(\tilde{x}(t), \tilde{\nu}(t), \eta(t))$ *remains bounded for all* $t \geq 0$ *and* $(\tilde{x}(t), \tilde{\nu}(t), \eta(t)) \to (\tilde{x}^*, \tilde{\nu}^*, \eta^*)$ *as* $t \to \infty$*, where* $(\tilde{x}^*, \tilde{\nu}^*, \eta^*)$ *is one equilibrium point in* $\mathbb{E}$.

Note that the initial condition of $\mathbb{I}$ requires only the cyber variables $\eta^-, \eta^+ \geq 0$. It is readily realizable since in practice they correspond to marginal congestion costs on lines that are always nonnegative in power markets. Remarkably, no initial condition is required on the power network states for the system to stabilize.

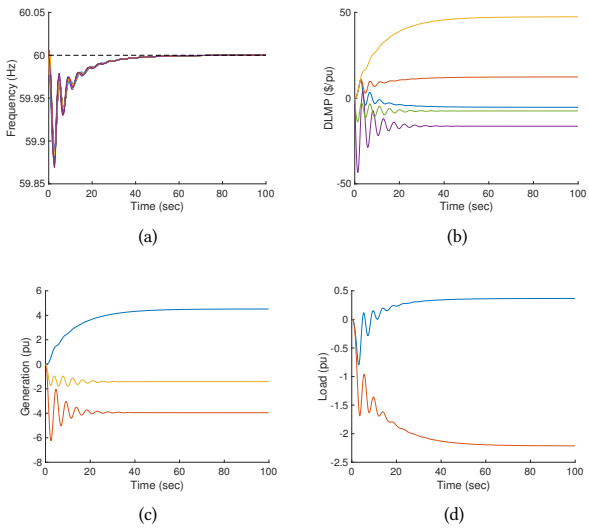

Figure 1: Dynamics of (a) frequencies; (b) dynamical locational marginal prices (DLMP); (c) generations; (d) loads.

4 NUMERICAL RESULTS

We test our market dynamics controller on the IEEE 39-bus system to illustrate its performance in secondary frequency control. Instead of the linear network model used for analysis, the numerical tests adopt a high-fidelity nonlinear setup including second-order turbine-governor dynamics, voltage dynamics and nonlinear power flows. Randomly we pick a subset of three generators (at buses 30, 32 and 34) and two loads (at buses 25 and 26) to participate in the *ex-post* power market, and impose 1 pu (100 MW) of step load increase at bus 30. Meanwhile, a subset of lines (#4, 19, 26) are endowed with relatively small capacities such that the line thermal constraints are binding. The efficacy of bus-variant DLMPs in guiding generators and loads to perform secondary frequency control is explicitly illustrated in Fig. 1. The market dynamics controller is able to drive the power network to a steady state within roughly 40 seconds.

5 CONCLUSION

In this work we propose to utilize market dynamics as a controller to stabilize power networks. Based on a linear model of swing equations, DLMPs that reflect temporal and spatial network states are designed in an *ex-post* power market to steer the rational dynamical behavior of generators and loads. We prove that the coupled system of power networks and market dynamics asymptotically converges to an equilibrium point that clears the market, restores the nominal frequency and maintains line flows within thermal limits. The performance of our controller is demonstrated through numerical tests on a nonlinear simulator.

ACKNOWLEDGMENT

This work was supported in part by NSFC under grant 61629302, the PNNL Lab Directed Research and Development Fund, and the PNNL Control of Complex Systems Initiative.

REFERENCES

[1] Fernando L Alvarado, Jianping Meng, Christopher L DeMarco, and Wellington S Mota. 2001. Stability analysis of interconnected power systems coupled with market dynamics. *IEEE Transactions on Power Systems* 16, 4 (2001), 695–701.

[2] Andrea Bacciotti and Francesca Ceragioli. 2006. Nonpathological Lyapunov functions and discontinuous Carathéodory systems. *Automatica* 42, 3 (2006), 453–458.

[3] Young Gyu Jin, Si Young Lee, Seung Wan Kim, and Yong Tae Yoon. 2013. Designing rule for price-based operation with reliability enhancement by reducing the frequency deviation. *IEEE Transactions on Power Systems* 28, 4 (2013), 4365–4372.

[4] Andrej Jokić, Mircea Lazar, and Paul PJ van den Bosch. 2009. Real-time control of power systems using nodal prices. *International Journal of Electrical Power & Energy Systems* 31, 9 (2009), 522–530.

[5] Arman Kiani and Anuradha Annaswamy. 2010. The effect of a smart meter on congestion and stability in a power market. In *49th IEEE Conference on Decision and Control (CDC)*. IEEE, 194–199.

[6] Prabha Kundur, Neal J Balu, and Mark G Lauby. 1994. *Power System Stability and Control*. Vol. 7. McGraw-hill New York.

[7] Na Li, Changhong Zhao, and Lijun Chen. 2016. Connecting automatic generation control and economic dispatch from an optimization view. *IEEE Transactions on Control of Network Systems* 3, 3 (2016), 254–264.

[8] Yile Liang, Feng Liu, and Shengwei Mei. 2015. Stability analysis of the hybrid dynamics coupling power systems with power markets. In *IEEE Power & Energy Society General Meeting*. IEEE, 1–5.

[9] Enrique Mallada, Changhong Zhao, and Steven Low. 2017. Optimal load-side control for frequency regulation in smart grids. *IEEE Transactions on Automatic Control* 62, 12 (2017), 6294–6309.

[10] Wellington S Mota and Fernando L Alvarado. 2001. Dynamic coupling between power markets and power systems with congestion constraints. In *IEEE Porto Power Tech Proceedings*, Vol. 1. IEEE, 1–6.

[11] John ZF Pang, Linqi Guo, and Steven H Low. 2017. Optimal load control for frequency regulation under limited control coverage. In *IREP Symposium*. 1–7.

[12] Tjerk Stegink, Claudio De Persis, and Arjan van der Schaft. 2017. A unifying energy-based approach to stability of power grids with market dynamics. *IEEE Transactions on Automatic Control* 62, 6 (2017), 2612–2622.

[13] Tjerk W Stegink, Claudio De Persis, and Arjan J van der Schaft. 2016. Stabilization of structure-preserving power networks with market dynamics. *arXiv preprint arXiv:1611.04755* (2016).

[14] Zhaojian Wang, Feng Liu, Steven H Low, Changhong Zhao, and Shengwei Mei. 2017. Distributed frequency control with operational constraints, part I: Per-node power balance. *IEEE Transactions on Smart Grid* (2017).

[15] Zhaojian Wang, Feng Liu, Steven H Low, Changhong Zhao, and Shengwei Mei. 2017. Distributed frequency control with operational constraints, part II: Network power balance. *IEEE Transactions on Smart Grid* (2017).

[16] David Watts and Fernando L Alvarado. 2004. The influence of futures markets on real time price stabilization in electricity markets. In *37th Annual Hawaii International Conference on System Sciences*. IEEE, 1–7.

[17] Changhong Zhao, Enrique Mallada, Steven Low, and Janusz Bialek. 2016. A unified framework for frequency control and congestion management. In *Power Systems Computation Conference (PSCC)*. IEEE, 1–7.

[18] Changhong Zhao, Ufuk Topcu, Na Li, and Steven Low. 2014. Design and stability of load-side primary frequency control in power systems. *IEEE Transactions on Automatic Control* 59, 5 (2014), 1177–1189.

[19] Changhong Zhao, Ufuk Topcu, and Steven Low. 2012. Swing dynamics as primal-dual algorithm for optimal load control. In *IEEE 3rd International Conference on Smart Grid Communications (SmartGridComm)*. IEEE, 570–575.

A APPENDIX

A.1 Derivation of B

Here all variables are in their nominal values. Deviations will be represented by adding Δ. Consider the generic expression for a real line flow P_{jk}:

$$P_{jk} = |V_j||V_k|\left(-g_{jk}\cos(\theta_j-\theta_k) - b_{jk}\sin(\theta_j-\theta_k)\right) \tag{12}$$

where $g_{jk} := \frac{r_{jk}}{r_{jk}^2+x_{jk}^2}$ and $b_{jk} := \frac{-x_{jk}}{r_{jk}^2+x_{jk}^2}$ denote the corresponding conductance and susceptance of line (j,k), respectively. Since we assume $r_{jk}=0$, (12) reduces to

$$P_{jk} = \frac{|V_j||V_k|}{x_{jk}}\sin(\theta_j-\theta_k) \tag{13}$$

If there is a small disturbance $\Delta\theta$ in bus phase angles, the line flow evolves accordingly:

$$P_{jk}+\Delta P_{jk} = \frac{|V_j||V_k|}{x_{jk}}\sin((\theta_j+\Delta\theta_j)-(\theta_k+\Delta\theta_k)) \tag{14}$$

By applying the Taylor series to the right-hand side at the nominal phase angles and ignoring the high-order terms, we can rewrite (14) as

$$P_{jk}+\Delta P_{jk} = \frac{|V_j||V_k|}{x_{jk}}\left[\sin(\theta_j-\theta_k)+\cos(\theta_j-\theta_k)(\Delta\theta_j-\Delta\theta_k)\right] \tag{15}$$

Combining (13) and (15) leads to the linearized line flow model in (1):

$$\Delta P_{jk} = \frac{|V_j||V_k|}{x_{jk}}\cos(\theta_j-\theta_k)(\Delta\theta_j-\Delta\theta_k) \tag{16}$$

i.e., $B_{jk} := \frac{|V_j||V_k|}{x_{jk}}\cos(\theta_j-\theta_k)$. □

A.2 Proof of Theorem 3.1

By assumption, there exists an finite solution to EDP-3. Since all its constraints are affine, Slater's condition is satisfied and strong duality holds. The KKT conditions are then both sufficient and necessary to characterize the primal-dual optimal solutions to EDP-3. Therefore, (x^*, v^*, η^*) is primal-dual optimal if and only if

- *Primal feasibility*: (5b)-(5g).
- *Dual feasibility*: $\eta^{-*}, \eta^{+*} \geq 0$.
- *Stationarity*: $\nabla_p L(x^*,v^*,\eta^*)=0$, $\nabla_d L(x^*,v^*,\eta^*)=0$, $\nabla_{\tilde{\theta}} L(x^*,v^*,\eta^*)=0$, $\nabla_\omega L(x^*,v^*,\eta^*)=0$.
- *Complementary slackness*: (7d), (7e).

The first two stationarity conditions give (7b), (7c). The third stationarity condition requires

$$\frac{\partial L}{\partial \tilde{\theta}_{jk}}(x^*,v^*,\eta^*) = B_{jk}(\mu_j^*-\mu_k^*)=0, \quad (j,k)\in\mathcal{E} \tag{17}$$

Considering $B_{jk}>0$, we have $\mu_j^*=\mu_k^*$, $(j,k)\in\mathcal{E}$. Since the graph $(\mathcal{N},\mathcal{E})$ is connected, naturally $\mu_j^*=\alpha$, $j\in\mathcal{N}$, where α is a constant. Meanwhile, the fourth stationarity condition implies

$$\frac{\partial L}{\partial \omega_j}(x^*,v^*,\eta^*) = D_j\omega_j^* - D_j\mu_j^* = 0, \quad j\in\mathcal{N} \tag{18}$$

Considering $D_j>0$, we have $\mu_j^*=\omega_j^*$, $j\in\mathcal{N}$. Therefore, $\omega_j=\alpha$, $j\in\mathcal{N}$, as well.

From (5e) and the above observation, summing up (5b)-(5d) over rows leads to $\sum_{j\in\mathcal{N}} D_j\omega_j = \alpha\sum_{j\in\mathcal{N}} D_j = 0$, which implies $\alpha=0$, i.e., $\mu^*=\omega^*=0$ as (7a) suggests. Therefore, the KKT conditions are fully captured in Theorem 3.1. □

A.3 Proof of Theorem 3.2

EDP-1 → EDP-2:

Given an optimal solution $(p^*, d^*, \theta^*_{\mathcal{N}^+})$ to EDP-1, assume (p^*, d^*) is not an optimal solution to EDP-2. Then there exists $(\hat{p},\hat{d})$ that satisfies (3b)-(3d) and meanwhile has a strictly smaller objective function value, i.e., $\sum_{j\in\mathcal{G}} J_j(\hat{p}_j) - \sum_{j\in\mathcal{N}^+} U_j(\hat{d}_j) < \sum_{j\in\mathcal{G}} J_j(p_j^*) - \sum_{j\in\mathcal{N}^+} U_j(d_j^*)$. Let $\hat{\theta}_{\mathcal{N}^+} := (\bar{C}B\bar{C}^T)^{-1}\hat{\pi}_{\mathcal{N}^+}$ with $\hat{\pi}_{\mathcal{G}} = r_{\mathcal{G}} + \hat{p} - \hat{d}_{\mathcal{G}}$ and $\hat{\pi}_{\mathcal{L}} = r_{\mathcal{L}} - \hat{d}_{\mathcal{L}}$. It is trivial to verify that $(\hat{p},\hat{d},\hat{\theta}_{\mathcal{N}^+})$ satisfies (2b)-(2e) and is thus feasible for EDP-1 with a strictly smaller objective

function value than $(p^*, d^*, \theta^*_{\mathcal{N}^+})$. However, this contradicts the fact that $(p^*, d^*, \theta^*_{\mathcal{N}^+})$ is optimal with respect to EDP-1. Therefore, (p^*, d^*) is an optimal solution to EDP-2.

EDP-2 → EDP-3:

Given an optimal solution (p^*, d^*) to EDP-2, assume $(p^*, d^*, \tilde{\theta}^* = \bar{C}^T(\bar{C}B\bar{C}^T)^{-1}\pi^*_{\mathcal{N}^+}, \omega^* = 0)$ is not an optimal solution to EDP-3. Then there exists $(\hat{p}, \hat{d}, \hat{\tilde{\theta}} = \bar{C}^T(\bar{C}B\bar{C}^T)^{-1}\hat{\pi}_{\mathcal{N}^+}, \hat{\omega} = 0)$ that satisfies (5b)-(5g) and meanwhile has a strictly smaller objective function value, namely, $\sum_{j\in\mathcal{G}} J_j(\hat{p}_j) - \sum_{j\in\mathcal{N}^+} U_j(\hat{d}_j) < \sum_{j\in\mathcal{G}} J_j(p^*_j) - \sum_{j\in\mathcal{N}^+} U_j(d^*_j)$. Note that $\tilde{\theta}$ is a function of p and d, thus $\hat{\tilde{\theta}}$ may still equal $\tilde{\theta}^*$ despite $(\hat{p}, \hat{d}) \neq (p^*, d^*)$. Apparently $(\hat{p}, \hat{d})$ satisfies (3b)-(3d) (the same as (5e)-(5g)) and is thus feasible for EDP-2 with a strictly smaller objective function value than (p^*, d^*). However, this contradicts the fact that (p^*, d^*) is optimal with respect to EDP-2. Therefore, $(p^*, d^*, \tilde{\theta}^* = \bar{C}^T(\bar{C}B\bar{C}^T)^{-1}\pi^*_{\mathcal{N}^+}, \omega^* = 0)$ is an optimal solution to EDP-3.

EDP-3 → EDP-1:

Given an optimal solution $(p^*, d^*, \tilde{\theta}^*, \omega^* = 0)$ to EDP-3, assume $(p^*, d^*, \theta^*_{\mathcal{N}^+})$ is not an optimal solution to EDP-1 for arbitrary $\theta^*_{\mathcal{N}^+}$ that satisfies $\tilde{\theta}^* = \bar{C}^T\theta^*_{\mathcal{N}^+}$. Then there exists $(\hat{p}, \hat{d}, \hat{\theta}_{\mathcal{N}^+})$ that satisfies (2b)-(2e) and meanwhile has a strictly smaller objective function value, i.e., $\sum_{j\in\mathcal{G}} J_j(\hat{p}_j) - \sum_{j\in\mathcal{N}^+} U_j(\hat{d}_j) < \sum_{j\in\mathcal{G}} J_j(p^*_j) - \sum_{j\in\mathcal{N}^+} U_j(d^*_j)$. Note that $\hat{\tilde{\theta}} := \bar{C}^T\hat{\theta}_{\mathcal{N}^+}$ may still equal $\tilde{\theta}^*$ despite $(\hat{p}, \hat{d}) \neq (p^*, d^*)$. It follows from (2b)-(2d) that $(\hat{p}, \hat{d}, \hat{\tilde{\theta}}, \hat{\omega} = 0)$ satisfies (5b)-(5d) and naturally (5e) by summing (5b)-(5d) up. Write $\hat{\theta}_{\mathcal{N}^+}$ in terms of $\hat{p}$ and $\hat{d}$ as $\hat{\theta}_{\mathcal{N}^+} = (\bar{C}B\bar{C}^T)^{-1}\hat{\pi}_{\mathcal{N}^+}$, where $\hat{\pi}_{\mathcal{G}} = r_{\mathcal{G}} + \hat{p} - \hat{d}_{\mathcal{G}}$ and $\hat{\pi}_{\mathcal{L}} = r_{\mathcal{L}} - \hat{d}_{\mathcal{L}}$, then it follows from (2e) that $(\hat{p}, \hat{d}, \hat{\tilde{\theta}}, \hat{\omega} = 0)$ also satisfies (5f), (5g). Therefore, $(\hat{p}, \hat{d}, \hat{\tilde{\theta}}, \hat{\omega} = 0)$ is feasible for EDP-3 with a strictly smaller objective function value than $(p^*, d^*, \tilde{\theta}^*, \omega^* = 0)$, which however is already optimal with respect to EDP-3. The contradiction indicates that $(p^*, d^*, \theta^*_{\mathcal{N}^+})$ is an optimal solution to EDP-1 for arbitrary $\theta^*_{\mathcal{N}^+}$ that satisfies $\tilde{\theta}^* = \bar{C}^T\theta^*_{\mathcal{N}^+}$. □

A.4 Proof of Theorem 3.3

Necessary condition:

Given an equilibrium point $(p^*, d^*, \theta^*, \omega^*, \lambda^*, \eta^{-*}, \eta^{+*})$, $\{\dot{\theta} = 0, \dot{\omega} = 0\} \leftrightarrow$ (7a), $\dot{p} = 0 \leftrightarrow$ (7b) and $\dot{d} = 0 \leftrightarrow$ (7c). Therefore, the stationarity conditions are satisfied.

With $\omega^* = \mu^* = 0$ and $\dot{\omega} = \dot{\mu} = 0$, (1b)-(1d) imply (5b)-(5d), respectively, if we set $\tilde{\theta}^* = C^T\theta^*$. In addition, $\dot{\lambda} = 0 \leftrightarrow$ (5e). By the definition of $[\cdot]^+_\eta$, $\dot{\eta}^- = 0$ and $\dot{\eta}^+ = 0$ imply (5f) and (5g), respectively. Therefore, the equilibrium point is primal feasible.

Note that the trajectory starts from an initial point in $\mathbb{I}$, then the definition of $[\cdot]^+_\eta$ enforces $\eta^-(t), \eta^+(t) \geq 0$ for all $t \geq 0$. On this basis, dual feasibility is guaranteed.

Finally, consider (5f) from primal feasibility. If the equality sign holds, (7d) is satisfied. If the strict less-than sign holds, η^- will be driven to 0, thus satisfying (7d) as well. A similar argument applies to (7e). Therefore, the complementary slackness conditions are also met.

From above, $(p^*, d^*, \tilde{\theta}^*, \omega^*, \mu^*, \lambda^*, \eta^{-*}, \eta^{+*})$ is a primal-dual optimal solution to EDP-3 by Theorem 3.1.

Sufficient condition:

Given a primal-dual optimal solution $(p^*, d^*, \tilde{\theta}^*, \omega^*, \mu^*, \lambda^*, \eta^{-*}, \eta^{+*})$ to EDP-3, as we have shown above, the stationarity conditions (7a)-(7c) imply $\dot{\theta} = 0$, $\dot{\omega} = 0$, $\dot{p} = 0$ and $\dot{d} = 0$. Then the primal feasibility condition (5e) implies $\dot{\lambda} = 0$. Finally, consider (5f): if the equality sign holds, $\dot{\eta}^- = 0$; if the strict less-than sign holds, $\eta^{-*} = 0$ according to the complementary slackness condition (7d), then still we have $\dot{\eta}^- = 0$. A similar argument applies to $\dot{\eta}^+ = 0$.

From above, $(p^*, d^*, \theta^*, \omega^*, \lambda^*, \eta^{-*}, \eta^{+*})$ is an equilibrium point. □

A.5 Proof of Theorem 3.5

We focus on the trajectories that start with initial points in $\mathbb{I}$. The whole proof boils down to the proofs of the following three statements:

Statement 1: Any trajectory $(\tilde{x}(t), \tilde{\nu}(t), \eta(t))$ converges to the largest invariant set that satisfies $\dot{V}(\tilde{x}(t), \tilde{\nu}(t), \eta(t)) = 0$ between the on-off switches of the projection $[\cdot]^+_\eta$.

Consider the following Lyapunov function

$$\begin{aligned} V(\tilde{x}, \tilde{\nu}, \eta) = &\frac{1}{2}(\tilde{x} - \tilde{x}^*)^T\Gamma^{\tilde{x}^{-1}}(\tilde{x} - \tilde{x}^*) \\ &+ \frac{1}{2}(\tilde{\nu} - \tilde{\nu}^*)^T\Gamma^{\tilde{\nu}^{-1}}(\tilde{\nu} - \tilde{\nu}^*) + \frac{1}{2}(\eta - \eta^*)^T\Gamma^{\eta^{-1}}(\eta - \eta^*) \end{aligned} \tag{19}$$

Its derivative with respect to time is

$$\begin{aligned} \dot{V}(\tilde{x}, \tilde{\nu}, \eta) &= -\nabla_{\tilde{x}}L(\tilde{x}, \tilde{\nu}, \eta)^T(\tilde{x} - \tilde{x}^*) + \nabla_{\tilde{\nu}}L(\tilde{x}, \tilde{\nu}, \eta)^T(\tilde{\nu} - \tilde{\nu}^*) \\ &\quad + \left[\nabla_\eta L(\tilde{x}, \tilde{\nu}, \eta)\right]^{+T}_\eta(\eta - \eta^*) \\ &\leq -\nabla_{\tilde{x}}L(\tilde{x}, \tilde{\nu}, \eta)^T(\tilde{x} - \tilde{x}^*) + \nabla_{\tilde{\nu}}L(\tilde{x}, \tilde{\nu}, \eta)^T(\tilde{\nu} - \tilde{\nu}^*) \\ &\quad + \nabla_\eta L(\tilde{x}, \tilde{\nu}, \eta)^T(\eta - \eta^*) \\ &\leq L(\tilde{x}^*, \tilde{\nu}, \eta) - L(\tilde{x}, \tilde{\nu}, \eta) + L(\tilde{x}, \tilde{\nu}, \eta) - L(\tilde{x}, \tilde{\nu}^*, \eta^*) \\ &= L(\tilde{x}^*, \tilde{\nu}, \eta) - L(\tilde{x}^*, \tilde{\nu}^*, \eta^*) + L(\tilde{x}^*, \tilde{\nu}^*, \eta^*) - L(\tilde{x}, \tilde{\nu}^*, \eta^*) \\ &\leq 0 \end{aligned} \tag{20}$$

The first equality applies (11). The second inequality holds due to the fact that $[y]^{+T}_u(u - u^*) \leq y^T(u - u^*)$ for arbitrary vectors y, u and $u^* \geq 0$. The third inequality arises from the convexity of $L(\tilde{x}, \tilde{\nu}, \eta)$ with respect to $\tilde{x}$ and its concavity with respect to $(\tilde{\nu}, \eta)$. The last inequality holds since the equilibrium point $(\tilde{x}^*, \tilde{\nu}^*, \eta^*)$ is also a saddle point of $L(\tilde{x}, \tilde{\nu}, \eta)$.

Define the largest invariant set between the on-off switches of the projection $[\cdot]^+_\eta$ by

$$\mathbb{S} := \left\{(\tilde{x}, \tilde{\nu}, \eta) \mid \dot{V}(\tilde{x}(t), \tilde{\nu}(t), \eta(t)) = 0,\ t \in \mathbb{R}_+\backslash\mathbb{T}\right\} \tag{21}$$

where $\mathbb{T}$ consists of all the time epochs when the projections switch between on and off. Since the Lyapunov function is radially unbounded, all trajectories will remain bounded. Moreover, as per the invariance principle for Caratheodory systems [2], $(\tilde{x}(t), \tilde{\nu}(t), \eta(t))$ converges to $\mathbb{S}$ as $t \to \infty$.

Statement 2: Any trajectory $(\tilde{x}(t), \tilde{\nu}(t), \eta(t))$ in the invariant set $\mathbb{S}$ is an equilibrium point of the closed-loop system (1) and (4), i.e., $\mathbb{S} \subseteq \mathbb{E}$.

For any trajectory $(\tilde{x}(t), \tilde{\nu}(t), \eta(t)) \in \mathbb{S}$, $\dot{V}(\tilde{x}(t), \tilde{\nu}(t), \eta(t)) = 0$ enforces

$$L(\tilde{x}(t), \tilde{\nu}^*, \eta^*) = L(\tilde{x}^*, \tilde{\nu}^*, \eta^*) = L(\tilde{x}^*, \tilde{\nu}(t), \eta(t)) \tag{22}$$

Differentiating the first equality of (22) with respect to time leads to

$$\begin{aligned}\dot{L}(\tilde{x}(t),\tilde{\nu}^*,\eta^*) &= \nabla_{\tilde{x}} L(\tilde{x}(t),\tilde{\nu}^*,\eta^*)^T \dot{\tilde{x}} \\ &= -\nabla_{\tilde{x}} L(\tilde{x}(t),\tilde{\nu}^*,\eta^*)^T \Gamma^{\tilde{x}} \nabla_{\tilde{x}} L(\tilde{x}(t),\tilde{\nu}^*,\eta^*) \\ &= 0\end{aligned} \tag{23}$$

Since $\Gamma^{\tilde{x}}$ is positive definite, $\nabla_{\tilde{x}} L(\tilde{x}(t),\tilde{\nu}^*,\eta^*) = 0$. Therein

$$\begin{aligned}&\nabla_{\tilde{\theta}} L(\tilde{x}(t),\tilde{\nu}^*,\eta^*) \\ &= B(C_{\mathcal{G}}^T \mu_{\mathcal{G}}^* + C_{\mathcal{L}}^T \mu_{\mathcal{L}}^*(\tilde{x}(t),\tilde{\nu}^*,\eta^*) + C_0^T \mu_0^*(\tilde{x}(t),\tilde{\nu}^*,\eta^*)) \\ &= 0\end{aligned} \tag{24}$$

and also note that $[C_{\mathcal{L}}^T, C_0^T]$ is full column rank as well as $\mu_{\mathcal{G}}^* = 0$, we obtain $\mu_{\mathcal{L}}^*(\tilde{x}(t),\tilde{\nu}^*,\eta^*) = 0$ and $\mu_0^*(\tilde{x}(t),\tilde{\nu}^*,\eta^*) = 0$. In addition, from (9) $\mu_{\mathcal{L}}^*(\tilde{x}(t),\tilde{\nu}(t),\eta(t))$ and $\mu_0^*(\tilde{x}(t),\tilde{\nu}(t),\eta(t))$ actually depend only on $\tilde{x}(t)$, i.e.,

$$\begin{aligned}&\nabla_{\tilde{\nu}} \mu_{\mathcal{G}}^*(\tilde{x}(t),\tilde{\nu}(t),\eta(t)) = 0, \quad \nabla_{\eta} \mu_{\mathcal{G}}^*(\tilde{x}(t),\tilde{\nu}(t),\eta(t)) = 0 \\ &\nabla_{\tilde{\nu}} \mu_0^*(\tilde{x}(t),\tilde{\nu}(t),\eta(t)) = 0, \quad \nabla_{\eta} \mu_0^*(\tilde{x}(t),\tilde{\nu}(t),\eta(t)) = 0\end{aligned} \tag{25}$$

which implies $\mu_{\mathcal{L}}^*(\tilde{x}(t),\tilde{\nu}(t),\eta(t)) \equiv \mu_{\mathcal{L}}^* = 0$ and $\mu_0^*(\tilde{x}(t),\tilde{\nu}(t),\eta(t)) \equiv \mu_0^* = 0$.

From above, $\nabla_p L(\tilde{x}(t),\tilde{\nu}^*,\eta^*) = 0$ and $\nabla_d L(\tilde{x}(t),\tilde{\nu}^*,\eta^*) = 0$ directly indicate

$$\begin{aligned}p_j(t) \equiv p_j^* &= J_j'^{-1}(\lambda^* - \mu_j^* + H_j\eta^{-*} - H_j\eta^{+*}), \quad j \in \mathcal{G} \\ d_j(t) \equiv d_j^* &= U_j'^{-1}(\lambda^* - \mu_j^* + H_j\eta^{-*} - H_j\eta^{+*}), \quad j \in \mathcal{N}^+\end{aligned} \tag{26}$$

Similarly, differentiating the second equality of (22) with respect to time leads to

$$\begin{aligned}&\nabla_{\tilde{\nu}} L(\tilde{x}^*,\tilde{\nu}(t),\eta(t))^T \Gamma^{\tilde{\nu}} \nabla_{\tilde{\nu}} L(\tilde{x}^*,\tilde{\nu}(t),\eta(t)) \\ &+ \nabla_{\eta} L(\tilde{x}^*,\tilde{\nu}(t),\eta(t))^T \Gamma^{\eta} \left[\nabla_{\eta} L(\tilde{x}^*,\tilde{\nu}(t),\eta(t))\right]_{\eta}^+ = 0\end{aligned} \tag{27}$$

Since both $\Gamma^{\tilde{\nu}}$ and Γ^{η} are positive definite and the second term on the left-hand side is nonnegative, we obtain $\nabla_{\tilde{\nu}} L(\tilde{x}^*,\tilde{\nu}(t),\eta(t)) = 0$. Therein

$$\begin{aligned}\nabla_{\lambda} L(\tilde{x}^*,\tilde{\nu}(t),\eta(t)) &= -\mathbf{1}_{\mathcal{G}}^T(r_{\mathcal{G}} + p^* - d_{\mathcal{G}}^*) - \mathbf{1}_{\mathcal{L}}^T(r_{\mathcal{L}} - d_{\mathcal{L}}^*) - r_0 \\ &= -\mathbf{1}_{\mathcal{G}}^T(r_{\mathcal{G}} + p(t) - d_{\mathcal{G}}(t)) - \mathbf{1}_{\mathcal{L}}^T(r_{\mathcal{L}} - d_{\mathcal{L}}(t)) - r_0 \\ &= \frac{\dot{\lambda}}{\gamma^{\lambda}} \\ &= 0\end{aligned} \tag{28}$$

As a consequence, $\dot{\lambda} = 0$ and $\lambda(t) \equiv \hat{\lambda}$ for some constant $\hat{\lambda}$. Moreover, $\nabla_{\mu_{\mathcal{G}}} L(\tilde{x}^*,\tilde{\nu}(t),\eta(t)) = 0$ implies

$$r_{\mathcal{G}} + p^* - d_{\mathcal{G}}^* - D_{\mathcal{G}}\mu_{\mathcal{G}}(t) - C_{\mathcal{G}}B\tilde{\theta}^* = 0 \tag{29}$$

and the minimizers $\mu_{\mathcal{L}}^*(\tilde{x}^*,\tilde{\nu}(t),\eta(t))$ and $\mu_0^*(\tilde{x}^*,\tilde{\nu}(t),\eta(t))$ of (9) imply

$$\begin{aligned}r_{\mathcal{L}} - d_{\mathcal{L}}^* - D_{\mathcal{L}}\mu_{\mathcal{L}}^* - C_{\mathcal{L}}B\tilde{\theta}^* &= 0 \\ r_0 - D_0\mu_0^* - C_0B\tilde{\theta}^* &= 0\end{aligned} \tag{30}$$

Summing up (29) and (30) and comparing with (28) readily yield $\mu_{\mathcal{G}}(t) \equiv \mu_{\mathcal{G}}^* = 0$. It follows from $\mu(t) = 0$ that $\dot{\tilde{\theta}} = C^T\mu(t) = 0$.

Last but not least, since $p(t) = p^*$ and $d(t) = d^*$, the term in the projection of (4b), $\beta := \underline{F} - H_{\mathcal{G}}^T(r_{\mathcal{G}} + p(t) - d_{\mathcal{G}}(t)) - H_{\mathcal{L}}^T(r_{\mathcal{L}} - d_{\mathcal{L}}(t)) \in \mathbb{R}^{|\mathcal{E}|}$, is also constant. Consider one arbitrary line $(j,k) \in \mathcal{E}$, if $\beta_{jk} > 0$, then $\dot{\eta}_{jk}^- > 0$ which indicates $\eta_{jk}^-(t) \to \infty$. This contradicts the fact that all trajectories are bounded and thus $\beta_{jk} \le 0$. In the case of $\beta_{jk} = 0$, obviously $\dot{\eta}_{jk}^- \equiv 0$. In the other case of $\beta_{jk} < 0$, $\eta^-(t) \equiv 0$ is imposed according to the definition of the projection and the initial condition of $\mathbb{I}$. Again, $\dot{\eta}_{jk}^- \equiv 0$. A similar argument yields $\dot{\eta}_{jk}^+ \equiv 0$ correspondingly.

So far we have shown any trajectory $(\tilde{x}(t),\tilde{\nu}(t),\eta(t)) \in \mathbb{S}$ satisfies $\dot{\tilde{x}} = 0$, $\dot{\tilde{\nu}} = 0$ and $\dot{\eta} = 0$, and therefore $(\tilde{x}(t),\tilde{\nu}(t),\eta(t)) \in \mathbb{E}$, which implies $\mathbb{S} \subseteq \mathbb{E}$.

Statement 3: Each trajectory $(\tilde{x}(t),\tilde{\nu}(t),\eta(t))$ literally converges to a single equilibrium point in $\mathbb{E}$.

As discussed above, $(\tilde{x}(t),\tilde{\nu}(t),\eta(t)) \to \mathbb{S}$ and $(\tilde{x}(t),\tilde{\nu}(t),\eta(t))$ remains bounded, thus there exists an infinite sequence of time epochs $\{t_k, k = 1,2,\dots\}$ such that as $k \to \infty$, $(\tilde{x}(t_k),\tilde{\nu}(t_k),\eta(t_k)) \to (\tilde{x}_S^*,\tilde{\nu}_S^*,\eta_S^*) \in \mathbb{S}$. This specific $(\tilde{x}_S^*,\tilde{\nu}_S^*,\eta_S^*)$ certainly lies in $\mathbb{E}$ and is used in the definition of the Lyapunov function $V(\cdot)$. Since $V(\cdot)$ is quadratic in $(\tilde{x}(t),\tilde{\nu}(t),\eta(t))$, it is lower bounded by $V(\tilde{x}_S^*,\tilde{\nu}_S^*,\eta_S^*) = 0$. Note that $V(\cdot)$ is nonincreasing in t, thus $V(t) \to V(\tilde{x}_S^*,\tilde{\nu}_S^*,\eta_S^*)$. Due to the continuities of $V(\cdot)$ in $(\tilde{x},\tilde{\nu},\eta)$ and $(\tilde{x}(t),\tilde{\nu}(t),\eta(t))$ in t, naturally $(\tilde{x}(t),\tilde{\nu}(t),\eta(t)) \to (\tilde{x}_S^*,\tilde{\nu}_S^*,\eta_S^*)$, i.e., $(\tilde{x}(t),\tilde{\nu}(t),\eta(t))$ converges to only one equilibrium point in $\mathbb{S} \subseteq \mathbb{E}$.

Conclusion: The above three statements jointly complete the proof of Theorem 3.5. □